



**AALBORG UNIVERSITY**  
DENMARK

**Aalborg Universitet**

## **RFID on the Road-Some Considerations About Passive Tag Antennas**

Franek, Ondrej; Kyritsi, Persefoni; Pedersen, Gert Frølund

*Published in:*

Proceedings of the 5th European Conference on Antennas and Propagation

*Publication date:*

2011

*Document Version*

Accepted author manuscript, peer reviewed version

[Link to publication from Aalborg University](#)

*Citation for published version (APA):*

Franek, O., Kyritsi, P., & Pedersen, G. F. (2011). RFID on the Road-Some Considerations About Passive Tag Antennas. In *Proceedings of the 5th European Conference on Antennas and Propagation* (pp. 1203-1207). IEEE.

### **General rights**

Copyright and moral rights for the publications made accessible in the public portal are retained by the authors and/or other copyright owners and it is a condition of accessing publications that users recognise and abide by the legal requirements associated with these rights.

- ? Users may download and print one copy of any publication from the public portal for the purpose of private study or research.
- ? You may not further distribute the material or use it for any profit-making activity or commercial gain
- ? You may freely distribute the URL identifying the publication in the public portal ?

### **Take down policy**

If you believe that this document breaches copyright please contact us at [vbn@aub.aau.dk](mailto:vbn@aub.aau.dk) providing details, and we will remove access to the work immediately and investigate your claim.

# RFID on the Road—Some Considerations About Passive Tag Antennas

Ondřej Franek\*, Persefoni Kyritsi†, Gert F. Pedersen\*

\*APNet Section, Department of Electronic Systems, Aalborg University

Niels Jernes Vej 12, DK-9220 Aalborg, Denmark

{of,gfp}@es.aau.dk

†European Patent Office

Landsbergerstr. 30, Munich 80339, Germany

pkyritsi@epo.org

**Abstract**—This paper presents an investigation of tag antenna performance in the scenario of a passive RFID tag placed on an asphalt road and inquired by readers in vehicles. Three types of antennas were chosen and their properties were studied for various dielectric properties of the asphalt paving. Water on the pavement (e.g. due to rainfall) was also taken into account, with various layer thicknesses. Based on the results of numerical experiments performed using the finite-difference time-domain (FDTD) method we demonstrate how the communication range between the tag and a reader varies depending on the materials surrounding the tag and wave polarization.

**Index Terms**—Antennas, RFID tags, road transportation

## I. INTRODUCTION

Radio frequency identification (RFID) is a technology that is based on miniature tags that can be attached to objects or persons. An *RFID tag* contains information associated with the object it is attached to. This information can be retrieved or even changed by dedicated devices called *RFID readers* that use radio signals to excite the tag and read out the information embedded in it. In that sense, RFID tags represent the evolution of bar codes by lifting the requirement for optical contact between the tag and the reader and allowing for storage and computation capabilities. However, RFID technology brings an additional qualitative leap as multiple tags can be networked and integrated through the readers into the digital world, thus leading to the “*Internet of things*” and the vision of built-in (also known as ambient / pervasive / ubiquitous) intelligence.

It is impossible to list all the applications where RFID technology has found use because they cover a vastly broad spectrum and because new applications arise every day. In principle any application involving identification and tracking is a candidate market for this technology: asset tracking and inventory management, manufacturing and supply chain automation, retail and warehouse control, people and livestock tracking, access control, timing and medical applications.

One of the first areas to see RFID systems deployed and widely used has been that of traffic and transportation systems [1]. We can broadly classify the system architecture into two possible scenarios:

- 1) *Reader on the road, tag in a vehicle*: each vehicle has a tag, just like today’s cars have license plates. This

allows for accurate identification and localization of the vehicles. This approach is used for example today in road pricing and toll systems [2].

- 2) *Reader in a vehicle, tag on the road*: tags are embedded in the infrastructure and are queried by readers in the vehicles. The infrastructure consists of road signs, crash barriers, toll posts and the pavement (road surface) itself. Having several tags embedded in the infrastructure and vehicles equipped with readers enables the dissemination of traffic related information and the structural monitoring of the infrastructure.

It is the case of RFID tags embedded in the road pavement that is of interest to us in the context of this paper. Our goal is to explore the radiation properties of RFID tags in the UHF frequency band (900 MHz) when the tags are embedded in asphalt and how these properties change as the humidity conditions change (e.g. layer of water on the road after a rainfall). We address this question with numerical simulations using the finite-difference time-domain (FDTD) method [3] applied to various tag antenna layouts.

This paper is structured as follows. Section II presents the description of the problem, the types of antennas and the setting of the numerical experiments. Section III shows the results in terms of mismatch loss, antenna efficiency and radiation patterns of the investigated antennas in various conditions. Section IV discusses the implications of the antenna properties on the reader-tag communication link budget. Finally, Section V summarizes this work and proposes design guidelines for placing RFID tags in the road pavement.

## II. PROBLEM DESCRIPTION

The subject of our study is an antenna affixed to a half-space of asphalt pavement which is covered by a layer of water of various thicknesses. The underlying and overlying materials are supposed to have a significant influence on the antenna performance and will contribute to the link budget. The dielectric properties of the asphalt pavement have, according to the literature, large variations depending on composition, porosity and water content [4]–[6]. To account for these variations, we changed the dielectric constant of the asphalt pavement  $\epsilon_r$  in

the range 2–12 and the conductivity  $\sigma$  in the range  $10^{-4}$ – $10^{-1}$  S/m. Furthermore, we assumed that a layer of water covers the pavement and has a thickness of up to 6 mm. The complex permittivity of the water was taken as  $80 - j4.156$  [7].

Three different planar antenna types were used in the investigation: a straight dipole, a meander dipole and a patch antenna (see Fig. 1a, b, c, respectively). The straight dipole of Fig. 1a is 76 mm long and 4 mm wide, with a 4 mm gap for attaching the RFID chip. The meander dipole spans 40 mm in length and 20 mm width. The patch antenna consists of a metal backed substrate with dimensions  $100 \times 100$  mm and thickness 2 mm, with a representative choice of material parameters taken as  $\epsilon_r = 10$ ,  $\sigma = 5$  mS/m, and a metallic patch on top of the substrate with dimensions  $48 \times 48$  mm. The patch is fed by a microstrip line connected to the edge of the patch and shorted at the side of the substrate to the ground plane. The antenna terminals were designed to accommodate a  $4 \times 4$  mm RFID chip, with internal resistance assumed  $10 \Omega$ .

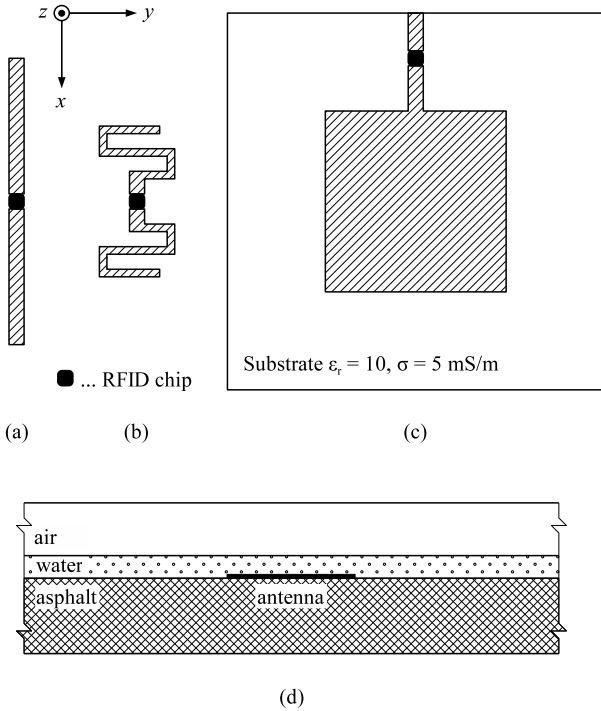


Fig. 1. RFID antenna geometries: a) dipole, b) meander dipole, c) patch antenna (metal backed); d) cross-section of the material layers near the antenna.

The antennas were tuned to resonance ( $\text{Im}(Z) = 0$ ) as close as possible to 900 MHz, for the pavement parameters  $\epsilon_r = 6$  and  $\sigma = 10^{-4}$  S/m, assuming no water layer. It should be noted that the imaginary part of the impedance of a typical RFID tag is seldom zero, unless the tag is equipped with a built-in matching circuit, and therefore, in a real situation, the antenna will have to be tuned to match a different, usually capacitive reactance corresponding to a particular tag. The decision to assume zero reactance for matching has been taken

for the sake of generality, as the variance of the typical tag capacitances is quite high.

The antennas were simulated using an FDTD code with complex frequency-shifted perfectly matched layers (PML) [3] as boundary conditions. The cell size was chosen to be 2 mm isotropic, so that the details of the antennas are accurately modeled and the numerical dispersion is kept at a minimum ensuring that there will always be at least 10 cells per wavelength even in the electrically densest material like water ( $\epsilon_r = 80$ ). The PML layers were 10 cells thick and positioned on all six domain boundaries, including those embedded entirely in asphalt, which means that possible reflections from the road bed underlying the asphalt were omitted for the sake of simplicity. The radiation pattern was calculated by a near-to-far-field transform [3] integrating over a surface positioned 8 mm above the asphalt-air boundary.

The computational domain extended 20 mm above and below the asphalt-air boundary, and to 2 m distance in each horizontal direction. The extreme size of the domain in horizontal directions was necessitated by the need to resolve the waves radiated under low elevation angles and to capture them into the radiation pattern. The cross-section of the computational domain near the antenna is shown in Fig. 1d.

### III. RESULTS

Fig. 2 shows variations of the mismatch loss (solid line) and the antenna efficiency (dashed line) when the relative permittivity of the asphalt pavement is set to 2, 4, 6, 8, 10, and 12, while the conductivity is kept at  $10^{-4}$  S/m. As expected, deviations of the permittivity of the underlying material from that of the substrate with  $\epsilon_r = 6$  detune the antennas off the resonance, the mismatch loss in dB increases for the dipole and the meander dipole. The antenna efficiency deteriorates monotonically with increasing permittivity as the dense dielectric material placed next to the antennas traps a high portion of fields within, and the material conductivity then dissipates the energy. Only the patch antenna, despite quite poor matching in the present setup, does not suffer from these effects, because it resides on a substrate isolating it from the influence of the asphalt. Similar observations can be made with Fig. 3, where the conductivity is varied in four steps,  $\sigma = 10^{-4}$ ,  $10^{-3}$ ,  $10^{-2}$ , and  $10^{-1}$  S/m, while the relative permittivity is fixed at  $\epsilon_r = 6$ .

When the pavement and the antennas are covered by a layer of water ( $\epsilon_r = 80$ ,  $\sigma = 0.2$  S/m [7]), as shown in Fig. 4, the detuning effect is the strongest. For higher water columns, however, we can observe that the mismatch loss is actually weaker, which seems contradictory at the first sight. In fact, the detuning is so strong here that the antennas are then tuned to their nearest higher resonance regimes. On the other hand, the antenna efficiency expectedly drops when the antennas are covered with a lossy material.

Fig. 5 shows the directivity of the dipole in two perpendicular planes: the E plane ( $x$ - $z$  plane in coordinate system of Fig. 1), corresponding to vertical polarization at the reader

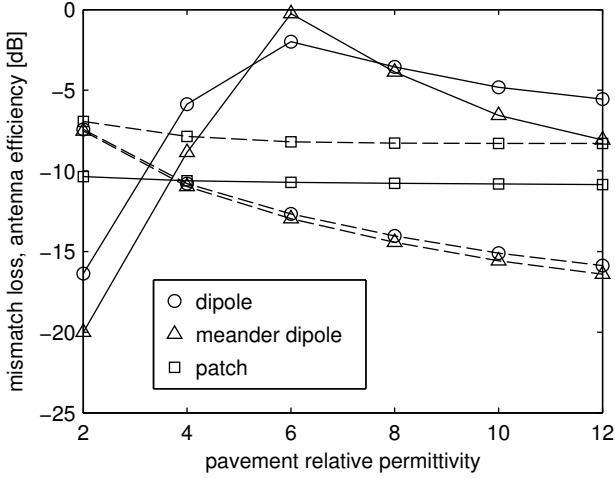


Fig. 2. Mismatch loss (solid line) and antenna efficiency (dashed line) as functions of relative permittivity of the asphalt pavement;  $\sigma = 10^{-4}$ .

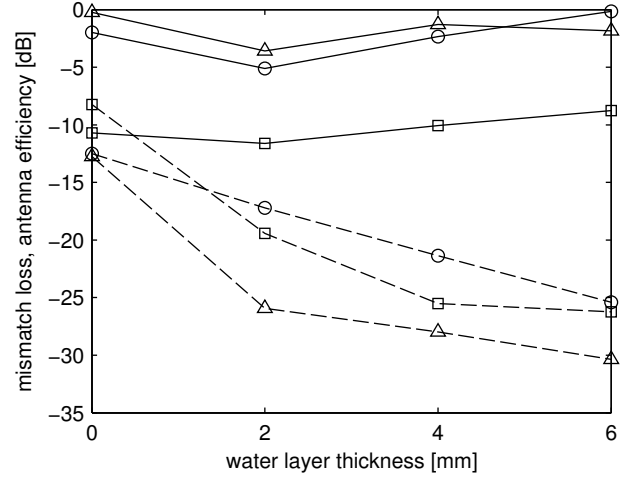


Fig. 4. Mismatch loss (solid line) and antenna efficiency (dashed line) as functions of thickness of the water layer. Pavement properties:  $\epsilon_r = 6$ ,  $\sigma = 10^{-4}$ . ( $\circ$  ... dipole,  $\triangle$  ... meander dipole,  $\square$  ... patch)

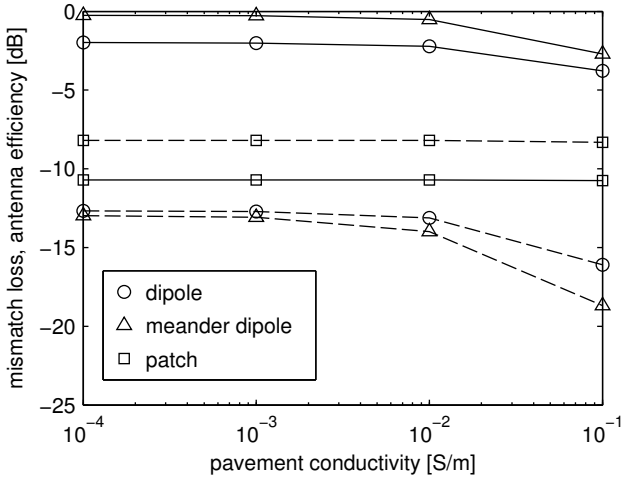


Fig. 3. Mismatch loss (solid line) and antenna efficiency (dashed line) as functions of conductivity of the asphalt pavement;  $\epsilon_r = 6$ .

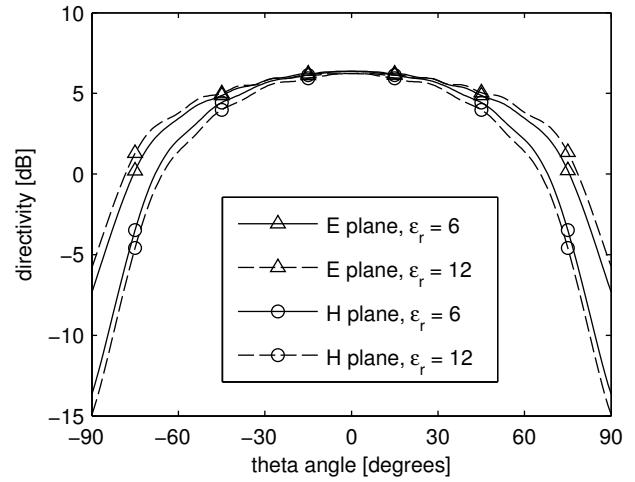


Fig. 5. Radiation patterns of the planar dipole antenna.

side (denoted by triangles), and the H plane ( $y$ - $z$  plane), corresponding to horizontal polarization for the reader (denoted by circles). The theta ( $\theta$ ) angle is taken from the  $z$ -axis normal to the pavement surface. Two curves for values 6 and 12 of the relative permittivity are shown for each plane. It is evident that the vertical polarization has increased directivity for higher angles of incidence, due to the presence of waves traveling along the asphalt-air interface. The gap between the polarizations even broadens when the asphalt has higher permittivity (e.g. when it is wet). The radiation patterns for the meander dipole and the patch antenna are almost identical.

Variations of the directivity with conductivity were generally negligible, and the corresponding graphs are not included. On the other hand, large variations occur when a water layer is added on top of the pavement, see Figs. 6–9. The solid, dashed, dash-dotted and dotted curves correspond to no layer of water, 2, 4, and 6 mm thick layers of water, respectively. Water on

the pavement surface distorts the radiation patterns, often in the order of 10 dB, due to severe detuning and, therefore, radically changed, nonoptimal mode of operation.

#### IV. DISCUSSION

Variations in mismatch loss, antenna efficiency and directivity have a strong impact on the quality of the communication and powering link between a reader in the vehicle and the passive tag on the road, and will influence the operation range of the RFID system. According to [8], the communication range of a passive UHF RFID system is primarily limited by the power threshold of the tag, i.e. the smallest power level capable of powering up the tag chip, as the sensitivity of the reader is usually very high. The power delivered to the tag is given by the Friis formula

$$P_{\text{tag}} = P_t G_t \left( \frac{\lambda}{4\pi R} \right)^2 G_r \eta \tau \quad (1)$$

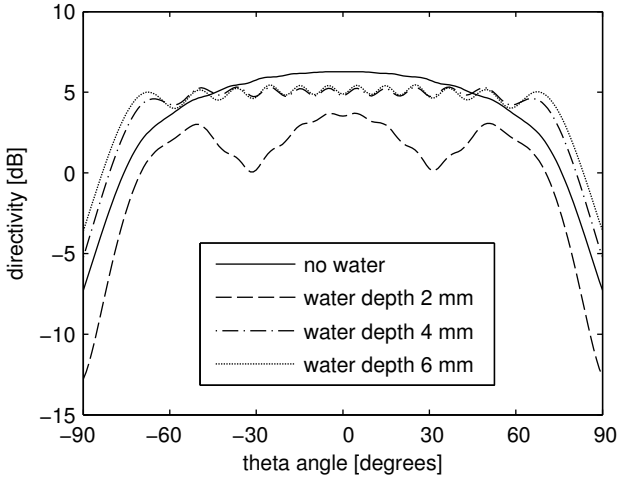


Fig. 6. Radiation patterns for the meander dipole antenna in E plane, for various water layer thicknesses.

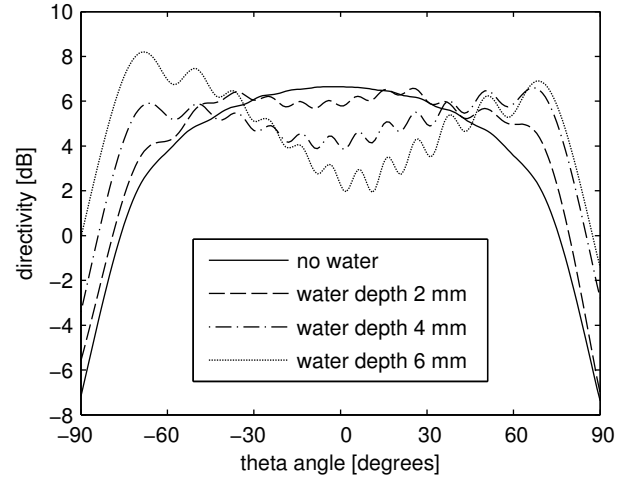


Fig. 8. Radiation patterns for the patch antenna in E plane, for various water layer thicknesses.

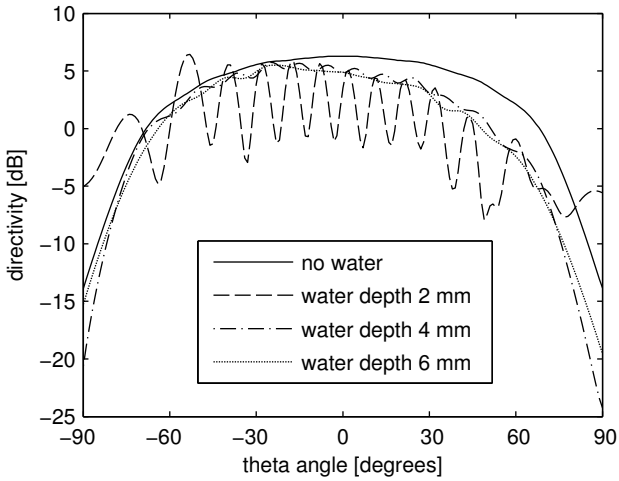


Fig. 7. Radiation patterns for the meander dipole antenna in H plane, for various water layer thicknesses.

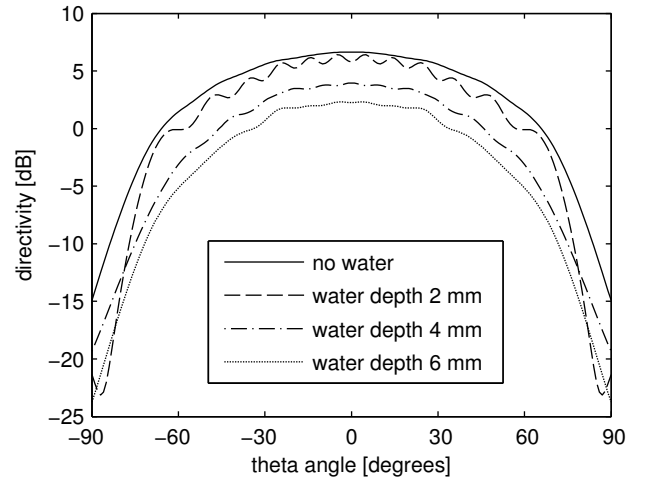


Fig. 9. Radiation patterns for the patch antenna in H plane, for various water layer thicknesses.

where  $P_t$  is the power transmitted by the reader,  $G_t$  is the gain of the reader antenna,  $\lambda$  is the wavelength,  $R$  is the distance between the reader and the tag antennas,  $G_r$  is the tag antenna directive gain,  $\eta$  is the tag antenna efficiency, and  $\tau$  is the mismatch loss between the tag and its antenna. Polarization losses are omitted in this formula, because the polarizations of the tag and the reader antennas are supposed to be matched—a vehicle will approach the tag mainly from the direction of the road lane, with substantial deviation only in close proximity to the tag, where, anyway, the field strength is expected to be sufficient to power the tag.

Let us consider the situation of a vehicle equipped with a reader that is approaching a dipole tag, placed on the road pavement (Fig. 10). The reader is mounted at a height of  $h = 0.5$  m and its horizontal distance from the tag is  $d$ , so that  $R = \sqrt{h^2 + d^2}$  and also  $R = h / \cos \theta$ , where  $\theta$  is the angular argument of the radiation patterns.

For a frequency of 900 MHz and effective radiated isotropic power (EIRP)  $P_t G_t$  of 3.28 W (we assume that the reader antenna has an omnidirectional radiation pattern), the power received by the tag as a function of  $d$  is shown in Fig. 11. In this figure, the four curves represent, similarly to Fig. 5, both polarizations and two values (6 and 12) of asphalt permittivity. The mismatch loss and antenna efficiency are not included, however, they would shift the received power down according to the appropriate values from Figs. 2–4.

In Fig. 11, the dotted line at  $-10$  dBm marks typical power threshold for passive tag chips. Using this threshold, selecting vertical polarization and assuming asphalt permittivity  $\epsilon_r = 6$  gives us a practical window for tag communication of approx. 7 m. If the speed of the vehicle does not exceed 200 km/h (124 mph), the reader will have 126 ms time window to interrogate the passive tag. This interval has to cover both directions of communication between the tag and the reader,



Fig. 10. RFID tag on the road scenario.

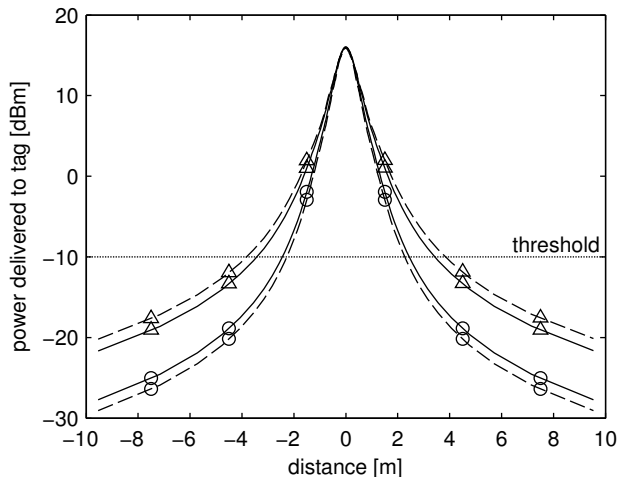


Fig. 11. Power delivered to the RFID tag on the road versus distance of the reader. (Pavement permittivity: solid line  $\epsilon_r = 6$ , dashed line  $\epsilon_r = 12$ ; Polarization:  $\Delta$  ... vertical,  $\circ$  ... horizontal)

and also the initial powering stage for waking up the tag chip, thus posing a limitation on the total amount of data transferred in either direction. Chon et al. [9] demonstrated tag transaction as short as 18 ms for a data size of 128 bit of the tag, which proves feasibility of the scenario even for larger data transfers.

Nevertheless, as already mentioned, the situation may be further deteriorated by the mismatch loss and antenna efficiency, see Figs. 2–4, perhaps even beyond the point of no connection at all. Table I presents achievable communication ranges and corresponding time windows when a tag with dipole antenna and vertical polarization is attached to asphalt pavement of varying permittivity and constant conductivity  $\sigma = 10^{-4}$ , and when mismatch loss and antenna efficiency are included in the calculation. Here, the lengths of the communication windows are not so favorable anymore, for asphalt with  $\epsilon_r = 2$  even lower than the 18 ms transaction limit. It is therefore necessary to design the antenna to be well matched to the impedance of the tag chip and, at the same time, try to isolate the effects of the changing surrounding environment (asphalt pavement dielectric parameters, water layer) by embedding the tag in protective coating. The length of the communication window may also be improved by increasing the directivity of the tag antenna for high angles of incidence, e.g. by adding parasitic elements to the dipole radiator.

TABLE I  
RANGES AND TIME WINDOWS FOR DIPOLE TAG, VERTICAL POLARIZATION.

$\epsilon_r$	Range [m]	Time window [ms]
2	0.57	10.3
4	1.75	31.4
6	2.20	39.6
8	1.67	30.1
10	1.32	23.7
12	1.04	18.7

## V. CONCLUSION

RFID reader-tag communication and powering link is negatively influenced by changes of the surrounding environment, in this case the asphalt pavement below the antenna and the water layer on top of it. However, the experiments have also shown that the influence of the pavement can be mitigated when the antenna is isolated from its underlying material, as in the case of the patch antenna with a dielectric substrate. Furthermore, the extra loss added by the water layer may be partly compensated by higher gain at higher angles of incidence for certain antenna configurations. It has also been found that for the reader-tag transmission vertical polarization is preferable, supposedly due to better propagation along the asphalt-air interface. If all these characteristics are taken into account and the system is carefully designed, the described scenario of the tag embedded in asphalt and the reader in a vehicle shows sufficient interrogation ranges even with today's RFID technology.

## ACKNOWLEDGMENT

This work was supported by the Danish Center for Scientific Computing. The authors would also like to thank prof. J. B. Andersen for reviewing the manuscript.

## REFERENCES

- [1] K. Finkenzeller, *RFID Handbook*, 2nd ed. Chichester: John Wiley & Sons, 2003.
- [2] P. Blythe, "RFID for road tolling, road-use pricing and vehicle access control," *IEEE Seminar Digests*, vol. 1999, no. 123, pp. 8–8, 1999. [Online]. Available: <http://link.aip.org/link/abstract/IEESEM/v1999/i123/p8/s1>
- [3] A. Taflov, *Computational Electrodynamics: The Finite-Difference Time-Domain Method*, 3rd ed. Boston: Artech House, 2005.
- [4] R. Evans, M. Frost, M. Stonecliffe-Jones, and N. Dixon, "Assessment of in situ dielectric constant of pavement materials," *Transportation Research Record: Journal of the Transportation Research Board*, vol. 2037, pp. 128–135, 2007.
- [5] J. Shang, "Effects of asphalt pavement properties on complex permittivity," *International Journal of Pavement Engineering*, vol. 3, no. 4, pp. 217–226, 2002.
- [6] E. Jaselskis, J. Grigas, and A. Brilingas, "Dielectric properties of asphalt pavement," *Journal of Materials in Civil Engineering*, vol. 15, no. 5, pp. 427–434, 2003.
- [7] A. Von Hippel, *Dielectric materials and applications*. Boston: Artech House, 1995.
- [8] P. Nikitin and K. Rao, "Performance limitations of passive UHF RFID systems," in *IEEE Antennas and Propagation Society International Symposium 2006*, 9–14 2006, pp. 1011–1014.
- [9] H. Chon, S. Jun, H. Jung, and S. An, "Using RFID for accurate positioning," *Journal of Global Positioning Systems*, vol. 3, no. 1–2, pp. 32–39, 2004.